V－13

TENSILE BEHAVIOR OF MULTI-MODAL FIBER REINFORCED CEMENT BASED COMPOSITES

Hokkaido University　○　Yasuhiko Sato
Delft University of Technology　Jan G. M. van Mier
Delft University of Technology　Joost.C.Walraven

1. Introduction

Recently, many studies on High Performance Fiber Reinforced Cement based Composites (HPFRCC) have been performed. Rossi (1) has developed a new composite with different steel fiber lengths, called High Performance Multi-modal Fiber Reinforced Cement based Composites (HPMFRCC).

The aim of this study is to make the HPMFRCC using materials available in the Dutch market and to clarify the strength and deformational characteristics of HPMFRCC by means of experimental observation, in which the length of fiber and volume fraction of fiber are chosen as an experimental parameter.

2. Introduction

2.1 Material and mixing composition

In this study, steel fibers with four different lengths were used as reinforcing material. The mechanical characteristics of the fibers are shown in ***Table 1***. The straight cylindrical fibers with 6, 13 and 20 mm in length were used as a short fiber and the cylindrical hocked fiber with 30 mm in length was used as long fiber.

Table 2 shows the mixing composition which has been developed based on previous study (1) and the properties of reference composite. From the reference matrix, the HPMFRCCs were obtained by replacing a volume of sand with the same volume of fibers. The aggregate used in the composites is very fine sand whose maximum and minimum particle sizes are 500 μ and 125 μ, respectively. As a binding material of composites, the blast furnace cement was used. The silica fume and the melamine type superplastisizer are also used.

Table 1　Properties of fibers

	Length (mm)	Diameter (mm)	Shape
A	6	0.16	Straight
B	13	0.16	Straight
C	20	0.5	Straight
D	30	0.5	Hook

Table 2　Composition of matrix for 1m^3

Cement	1013kg
Sand	704kg
Silica fume	253kg
Water	223kg
Superplasticizer	52kg
W/C	22.0%
S/C	25.0%

2.2 Mixing and casting

The mixing machine used is a pan mixer in which not only the mixing arms but also the pan itself can rotate. The mixing was performed as follows. First, the sand and silica fume were mixed up. Secondly, water containing the superplastisizer was poured into it. Thirdly, the cement was cast while the mixing continued until the slurry becomes homogeneous. Finally the fibers were slowly added to the matrix. The mix was cast in the moulds without any compulsory compacting. The matrix had good workability and compactivility as self-compacting concrete, except for series 7 shown in Table 3.

The specimens were allowed to harden at room temperature for 2 days prior to demolding and then were stored in the curing room whose temperature was 20℃ and 100% relative humidity until one day before the testing. The experiment was conducted at the age of between 24 and 30 days. The notch in the specimens had been prepared in two weeks after the casting.

2.3 Specimens and test program

In this study, experiments of eighteen series are performed (see Table 1). The experimental parameters are the length of short fiber and the amount of short and/or long fibers. The short fibers (Type A, B and C in Table 1) are used in volume fraction of 2, 4 and 6% and the long fiber (Type C in Table 2) is used in volume fraction of 1, 1.5 and 2 % in the same matrix. Tree notched I-shaped specimen with 140mm height and 40mm width (see ***Fig.1*** and ***2***) were prepared. In I-shaped specimen the cross sectional area is reduced toward the middle height of specimen and two saw cuts with 5mm or 10mm depth were prepared at the middle, in which the cross-sectional area is 30×30 mm for specimens in series 1 to 6, 8, 9 and two specimens in series 10 or 30×20 mm for specimens in series 11 to 14 and a rest in series 10. The details of specimens are shown in ***Table 3***. Specimens in series 1 have no fibers. Specimens in series 2 to 10 are reinforced with short fiber only. The difference in these specimens is the amount and/or length of short fibers. Using specimens 1 to 10, the influences of short fiber on mechanical characteristics of composites can be examined. The specimens in series 11 to 14 have both of short and long fibers. In these specimens, the length of short fiber was fixed at 6mm.

Table 3 Details of specimens

No	Short fiber		Long fiber	
	Length (mm)	Volume (%)	Length (mm)	Volume (%)
1	-	0	-	0
2	6	2	-	0
3	6	4	-	0
4	6	6	-	0
5	13	2	-	0
6	13	4	-	0
7	13	6	-	0
8	20	3	-	0
9	20	4	-	0
10	6	2	30	1.0
11	6	2	30	1.5
12	6	2	30	2.0
13	6	4	30	1.0
14	6	4	30	1.5

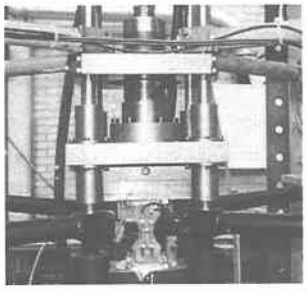

Fig.1 Test setup

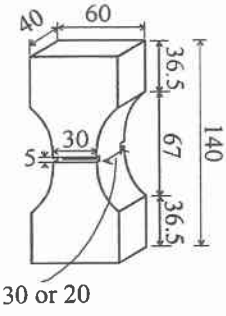

Fig.2 Specimen

The crack width at the middle of the specimen has been measured by means of LVDTs. Four LVDTs were set 50mm apart on front and back sides. In most of the 14 series, two specimens were tested under monotonic loading and the rest was tested under cyclic loading. Loading speed was fixed at 0.6 μ m/sec before the peak load and at 0.002mm/sec after the peak load.

3. Tensile characteristics

3.1 Failure mode

Figure 3 shows a typical cracked surface observed in specimens in series 1, 3 and 12. The crack plane in specimen with fiber has uneven surface because the crack would propagate through an area with no or less amount of fibers.

(a) Series 1

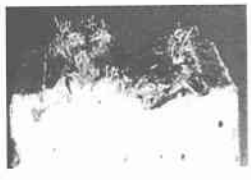

(b)Series 3

(c)Series 8

Fig.3 Cracked surface

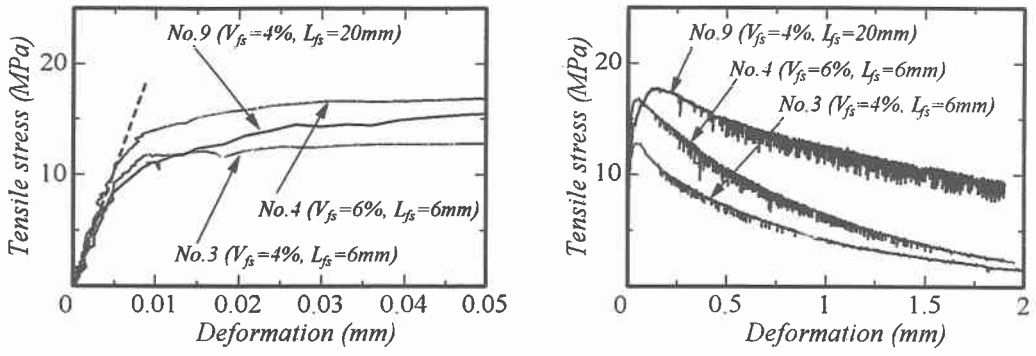

(a) until 0.05mm (b) until 2mm

Fig.4 Tensile stress – deformation curves

The stress-deformation curves observed in series 3, 4 and 9 are shown in ***Fig.4***. Typical response of fiber reinforced composite can be observed, i.e., the fiber gives a higher tensile strength and improved ductility as fiber length and volume fraction of fibers increase. Detail investigation on the tensile strength and the softening regime will be conducted.

3.2 Tensile strengths

Figure 5 shows the relationships between the maximum tensile stress and volume fraction of fiber for specimens without fiber and with short fiber only. Tensile strength greatly increases as the volume fraction of fiber becomes larger and as length of fiber becomes longer. The small scatter in a series with three specimens is observed. The relationships between maximum tensile stress and volume fraction of fiber for specimens with a combination of short and long fibers are shown in ***Fig.6***. The tensile strength becomes greater as volume fraction is greater as well but the significant scatter in a series exists.

The expected and observed volume fraction of fibers are shown in ***Table 4***. The volume fraction is calculated under the assumption that all fibers counted are oriented to the direction of loading. A significant difference between the expected and actual volume fraction is observed.

It is generally considered that the strength of a composite with short fiber linearly increases as the $V_f \cdot (L_f/d_f)$ becomes larger [2]. ***Fig.7*** shows the relationships between tensile strength and $V_f \cdot (L_f/d_f)$ for all specimens. For the specimens with a combination of short and long fibers, the observed volume fraction shown in Table 4 is used and the $V_f \cdot (L_f/d_f)$ is calculated by Eq.(1).

$$\frac{l}{d}V_f = \frac{l_s}{d_s}V_{fs} + \frac{l_l}{d_l}V_{fl} \tag{1}$$

whrere, where V_{fs} and V_{fL} are the volume fraction of short fiber and that of long fiber, L_{fs} and L_{fL} are the length of short fiber and that of long fiber, d_{fs} and d_{fL} are the diameter of short fiber and that of long fiber.

It can be said from *Fig.6* that the tensile strength observed lineally increases except for the case with 6mm fiber of 4% volume fraction. There is a possibility that an actual volume fraction in the cracked section of specimens with 6mm fiber of 4% is less than that expected one but it was impossible to count the number of short fibers by means of visually.

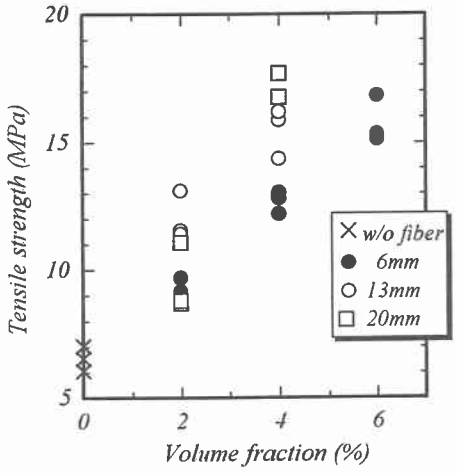

Fig.5 Relationships between tensile strength and volume fraction of fiber (with short fiber only)

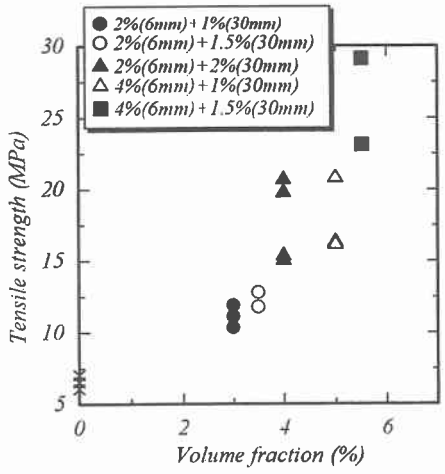

Fig.6 Relationships between tensile strength and volume fraction of fiber(with short and long fibers)

Table 4 The number of fibers observed

Series	Specimen	n	V_{fl}	V^*_{fl}
10	10-1	1.9	1	0.37
	10-2	2.9	1	0.57
	10-3	1.6	1	0.31
11	11-2	2.6	1.5	0.51
	11-3	2.1	1.5	0.41
12	12-1	5.1	2	1.00
	12-2	4.7	2	0.93
	12-3	13.0	2	2.56
	12-4	11.6	2	2.28
13	13-1	3.1	1	0.60
	13-2	4.9	1	0.96
	13-3	2.6	1	0.50
14	13-1	14.2	1.5	2.80
	13-2	10.1	1.5	2.00

n : number of fibers counted
V_{fl} : expected volume fraction of long fiber
V^*_{fl} : observed volume fraction of long fiber

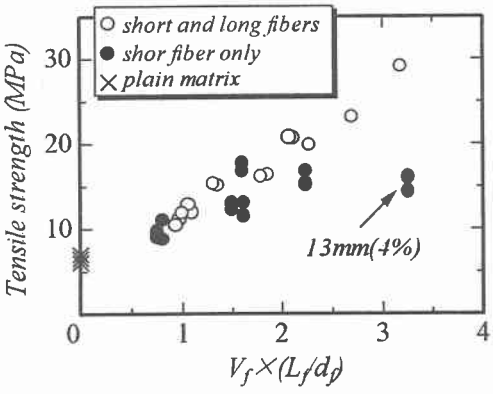

Fig.7 Relationships between compressive strength and $(L/d)V_f$

3.3 Softening regime

Figure 8 shows the relationships between stress normalized by tensile strength and fictitious crack width normalized by a half of fiber length for specimens with 6mm fiber only. The shape of softening regime does not change for different volume fraction of fibers. The average softening curves for different length of fiber are shown in ***Fig.9***. The shape of softening curve does not change for different length of fiber either.

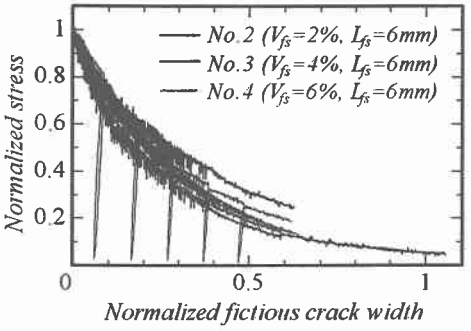

Fig.8 Normalized stress – normalized fictitious crack width curves for different volume fraction of fibers

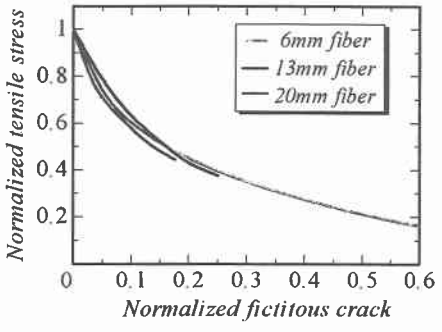

Fig.9 Normalized stress – normalized fictitious crack width curves for different fiber lengths

Figure 10 shows the relationships normalized stress and fictitious crack width in specimens with a combination of short and long fibers. The amount of long fiber gives better ductility than that with short fiber only. The amount of long fiber greatly affects the shape of the softening regime in tensile stress – crack width curve.

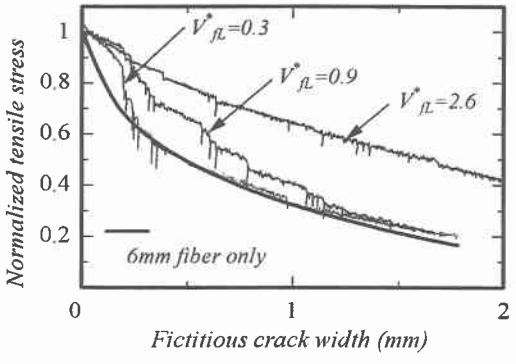

Fig.10 Normalized stress – fictitious crack width curves

The rate of the stiffness degradation of specimens during cyclic loading is shown in ***Fig.11***. The rate of stiffness degradation is given as the stiffness normalized by the slope connecting the maximum stress point and the origin in a stress-deformation curve. The stiffness decreases as crack width increase as shown in ***Fig.11***. The stiffness in specimen with 6mm fiber only is less than that in another specimens when the given crack width is the same.

Figure 12 shows the rate of stiffness degradation and energy accumulated until the crack width when an unloading starts. The energy is normalized by the total energy in which it is assumed that the tensile stress becomes zero at the crack width becomes a half of fiber length. It might be concluded that the unloading stiffness decreases linearly in relation to tensile stress normalized by the maximum tensile stress and crack width normalized by the half of fiber length.

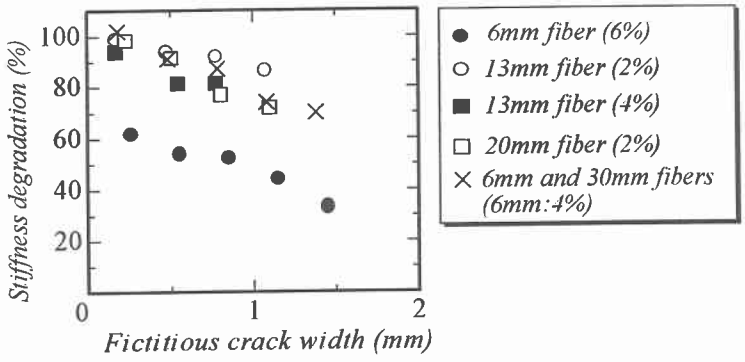

Fig.11 Relationships between stiffness degradation and fictitious crack width

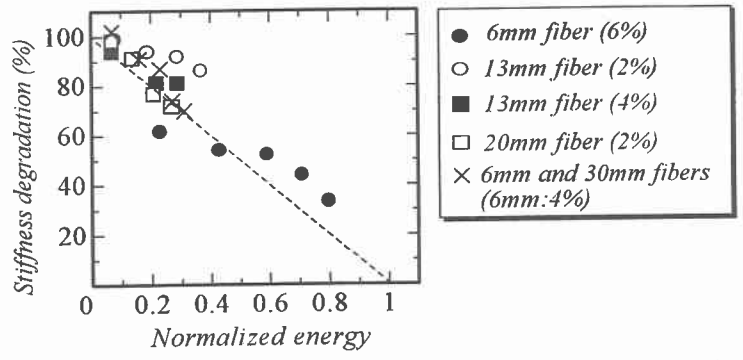

Fig.12 Relationships between stiffness degradation and normalized energy

5. Conclusion

The conclusions obtained from this study are shown as follows:

(1)The tension softening curve in specimens with shot fiber only does not change for different fiber lengths and volume fractions when the tensile stress and crack width are normalized by maximum tensile stress and a half of fiber length respectively.

(2) The amount of long fiber gives better ductility than that with short fiber only. The amount of long fiber greatly affects the shape of the softening regime in tensile stress – crack width curve.

(3)The unloading stiffness decreases linearly in relation to tensile stress normalized by the maximum tensile stress and crack width normalized by the half of fiber length.

6. References

1 P., Rossi and S., Renwez, 'High performance multimodal fiber reinforced cement composites', Proceedings of 4th international symposium on utilization of high-strength/high-performance concrete, 687-694(1996).

2 D., A., Fanella and A., E., Naaman, 'Stress-strain properties of fiber reinforced mortal in compression', ACI Journal, July-August, 475-483(1985).